PCP
PLANT & CELL PHYSIOLOGY

Regular Paper

Roles of the Cyclic Electron Flow Around PSI (CEF-PSI) and O_2-Dependent Alternative Pathways in Regulation of the Photosynthetic Electron Flow in Short-Term Fluctuating Light in *Arabidopsis thaliana*

Masaru Kono*, Ko Noguchi and Ichiro Terashima

Department of Biological Sciences, Graduate School of Science, The University of Tokyo, 7-3-1 Hongo, Bunkyo-ku, Tokyo, 113-0033 Japan
*Corresponding author: Email, konom07@biol.s.u-tokyo.ac.jp; Fax, +81-3-5841-4465.
(Received January 7, 2014; Accepted February 6, 2014)

To assess the roles of the cyclic electron flow around PSI (CEF-PSI) and O_2-dependent alternative pathways including the water–water cycle in fluctuating light, we grew the wild type and *pgr5* mutant of *Arabidopsis thaliana* in constant light, and measured Chl fluorescence and P700 parameters in their leaves in the fluctuating light alternating between 240 (HL) and 30 μmol photons $m^{-2} s^{-2}$ (LL) every 2 min. At 20% O_2, the photochemical quantum yield of PSII decreased, in particular in the *pgr5* plants, soon after the start of the fluctuating light treatment. PSI of the *pgr5* plants was markedly photoinhibited by this treatment for 42 min. Slight PSI photoinhibition was also observed in the wild type. We measured energy sharing between PSII and PSI and estimated the PSI and PSII electron transport rates (ETRs). *pgr5* showed larger energy allocation to PSI. In contrast to the wild type, the ratio of the PSI to the PSII ETR in *pgr5* was higher in LL but lower in HL at 20% O_2 due to PSI acceptor-side limitation. At 2.7% or 0% O_2, the CEF-PSI of the *pgr5* plants was enhanced, the acceptor-side limitation of PSI electron flow was released and PSI photoinhibition was not observed. The results suggest that the light fluctuation is a potent stress to PSI and that the CEF-PSI is essential to protect PSI from this stress.

Keywords: Alternative electron flow • Fluctuating light • PGR5 • Photoinhibition of PSI.

Abbreviations: ΔA_{max}, maximum level of P700 signal in the dark; CEF, cyclic electron flow; ETR, electron transport rate; FQR, ferredoxin-plastoquinone reductase; F_v/F_m, maximum quantum yield of PSII; HL, high light; LED, light-emitting diode; LEF, linear electron flow; LL, low light; NDH, NADH dehydrogenase-like complex; NPQ, non-photochemical quenching; PPFD, photosynthetic photon flux density; PTOX, plastid terminal oxidase; qE, energy-dependent quenching; qI, photoinhibitory quenching; qL, fraction of open PSII reaction centers; qT, state transition quenching; ROS, reactive oxygen species; SP, saturation pulse; WT, wild-type; WWC, water–water cycle.

Introduction

Even in open habitats, plants experience dynamic fluctuations of light because of clouds. Understorey plants experience more frequent, short-term light fluctuations due to leaves and stems of other plants above them in addition to clouds. Plants have to cope with these light fluctuations of various time ranges. In constant low light, plants can use most of the light energy in driving photochemistry. In contrast, in constant high light, energy transfer from antenna Chls to the PSII reaction center is suppressed and the excess energy is dissipated as heat. This process prevents photoinhibition. When the light intensity fluctuates between low and high levels very rapidly, however, it is not possible for chloroplasts to switch the heat dissipation system on and off synchronously with the light fluctuation because both induction and deactivation of the heat dissipation system require at least several minutes (Müller et al. 2001). Plants must have more rapid systems to cope with very rapid light fluctuations.

Photosynthetic electron transport primarily occurs via a linear pathway, in which electrons flow from water via PSII and the Cyt b_6/f complex to PSI and reduce $NADP^+$ to NADPH. The linear electron flow (LEF) generates the transmembrane electrochemical potential difference of H^+, through water splitting by PSII in the thylakoid lumen and translocation of H^+ across the thylakoid membrane by the Q cycle. The electrochemical potential difference thus produced drives the H^+-ATP synthase to produce ATP. Low pH in the thylakoid lumen causes de-epoxidation of violaxanthin to zeaxanthin via antheraxanthin and protonation of the PsbS protein, both of which contribute to the heat dissipation, which can be measured fluorometrically as the non-photochemical quenching (NPQ).

In addition to the LEF system, there are two PSI cyclic electron flow (CEF) systems (Shikanai 2007): the NADH dehydrogenase-like complex-dependent pathway (NDH-CEF; Burrows et al. 1998, Shikanai et al. 1998, Peng et al. 2011, Yamamoto et al. 2011) and the ferredoxin-plastoquinone reductase pathway (FQR-CEF; Munekage et al. 2002, Munekage et al. 2004, DalCorso et al. 2008, Hertle et al. 2013). FQR-CEF involves the

Plant Cell Physiol. 55(5): 990–1004 (2014) doi:10.1093/pcp/pcu033, available online at www.pcp.oxfordjournals.org

Cyt b_6/f complex, plastocyanin, PSI, ferredoxin (Fd) and FQR. PGR5 was identified as an essential component of the FQR-CEF (Munekage et al. 2002; see below). Very recently, PGRL1 has been proposed to be the elusive FQR (Hertle et al. 2013). In C_4 plants, the CEFs around PSI (CEF-PSI), particularly the NDH-CEF, operate to supply ATP to the CO_2-concentrating mechanism (Takabayashi et al. 2005) as well as the Calvin–Benson cycle. It is noteworthy that the NDH-CEF also involves ferredoxin (Okegawa et al. 2008, Johnson 2011, Yamamoto et al. 2011). It is often claimed that ATP and NADPH production by LEF cannot meet the required ATP/NADPH ratio for the photosynthetic carbon fixation by the Calvin–Benson cycle. In particular, when photorespiration occurs at high rates, the required ratio shifts from 3ATP/2NADPH towards 3.5ATP/2NADPH, and thereby shortage of ATP may be more serious (Allen 2002, Shikanai 2007). The CEF-PSI would contribute to producing additional ATP. Another function of CEF-PSI is enhancement of the NPQ, through generating the electrochemical potential difference of H^+ across the thylakoid membrane (Munekage et al 2002).

Pseudo-cyclic electron flow, also called the water–water cycle (WWC) (Asada 1999) or the Mehler–ascorbate peroxidase (MAP) pathway (Schreiber et al. 1995), is the electron flow from water via PSII, Cyt b_6/f and PSI to molecular oxygen. Since the redox potentials of the electron acceptors on the acceptor side of the PSI complex are sufficiently low to reduce O_2, electron flow to O_2 occurs, particularly when $NADP^+$ is not available. This results in the formation of reactive oxygen species (ROS), such as O_2^- and H_2O_2 (Asada 1999). Superoxide dismutase and ascorbate peroxidase in the WWC scavenge O_2^- and H_2O_2. NADPH is used to regenerate ascorbate from monodehydroascorbate or dehydroascorbate. Summing up these reactions, electrons are transferred from water to H_2O_2 to form water. Thus, the WWC acts as a large electron sink (Asada 2000). The WWC also generates the electrochemical potential difference of H^+ across the thylakoid membrane, which enhances the non-radiative dissipation of excess light energy observed as the increase in NPQ. Therefore, the WWC is also considered to play roles in dissipation of excess light energy (Osmond and Grace 1995, Osmond et al. 1997, Asada 1999, Asada 2000, Foyer and Noctor 2000, Miyake 2010). The CEF-PSI and WWC are thought to protect plants from damage that occurs due to the over-reduction of the thylakoids under stress conditions (Miyake 2010).

An *Arabidopsis thaliana* mutant, *pgr5* (*proton gradient regulation*), was reported to have impaired electron transfer in FQR-CEF (Munekage et al. 2002). In a screen using the Chl fluorescence imaging technique, this mutant showed a phenotype similar to that of *npq* mutants (Shikanai et al. 1999). NPQ measurements with this mutant showed an almost complete absence of energy-dependent quenching (qE) at high irradiance under steady-state photosynthesis (Munekage et al. 2002). Nandha et al. (2007), however, reported that the capacity for cyclic electron transport in *pgr5* was comparable with that of the wild-type (WT). They also showed that the electron transport system in *pgr5* was greatly reduced under most conditions.

A recent study has proposed an important role for PGR5 in protection of PSI under fluctuating growth light in *A. thaliana* (Suorsa et al. 2012). The *pgr5* mutant showed no growth when grown in drastically fluctuating light, alternating low light for 5 min and high light for 1 min (Tikkanen et al. 2010, Suorsa et al. 2012). In a more moderately fluctuating growth light, the PSI complex in this mutant was found to be photodamaged. These authors also reported that, under constant growth light, the *pgr5* mutant did not show any visible growth phenotype irrespective of the growth irradiance levels. From these findings, they argued that the *pgr5* could not maintain the redox balance of the electron transfer reactions in fluctuating light. However, how the redox imbalance occurs in *pgr5* and how the WT plants cope with the drastically fluctuating light are still unclear.

The aim of this study was to examine photosynthetic responses of WT and *pgr5* plants, both grown in continuous moderate light in the light period, to a fluctuating light using simultaneous Chl fluorescence and P700 measurements under the precise control of gas concentrations. The fluctuating light adopted was alternation of low light for 2 min and high light for 2 min. Even for high light, a moderate level of photosynthetically active photon flux density (PPFD) was chosen. We examined whether photoinhibition of PSI occurred in the mature leaves of the *pgr5* plants in short-term experiments for up to 42 min. Next, we tried to elucidate which of the photosynthetic alternative electron flows was impaired in the *pgr5* plants through examining the effects of O_2 concentrations at various PPFDs.

Results

Responses of PSII and PSI quantum yields to fluctuating and continuous light

Chl fluorescence and absorption changes at 830 nm in the intact leaf were measured simultaneously using a Dual-PAM-100 (Walt GmbH). Changes in the PSII quantum yield, Y(II), in mature leaves of the WT and *pgr5* plants were measured in the light regime that alternated between high light (HL) at 240 μmol photons $m^{-2}s^{-1}$ for 2 min and low light (LL) at 30 μmol photons $m^{-2}s^{-1}$ for 2 min, for a total of 42 min (**Fig. 1**). The leaf was kept in a small hand-made chamber, and CO_2 and O_2 gas concentrations in the chamber were regulated with mass-flow controllers. Unless otherwise stated, the CO_2 and O_2 concentrations were 390 p.p.m. and 20%, respectively. In the leaves of WT plants grown in the constant light at 90–100 μmol photons $m^{-2}s^{-1}$ for 8 h d^{-1}, Y(II) at the end of each LL period decreased with the cycle, but Y(II) at the end of each HL period did not change after attaining the steady value of around 0.45. In *pgr5*, Y(II) in the LL period decreased with the cycle more markedly than in the WT. Y(II) in the HL period also decreased after the fifth cycle. In the last cycle, Y(II) in the LL period became 0.4, approaching that in the HL period which was around 0.3.

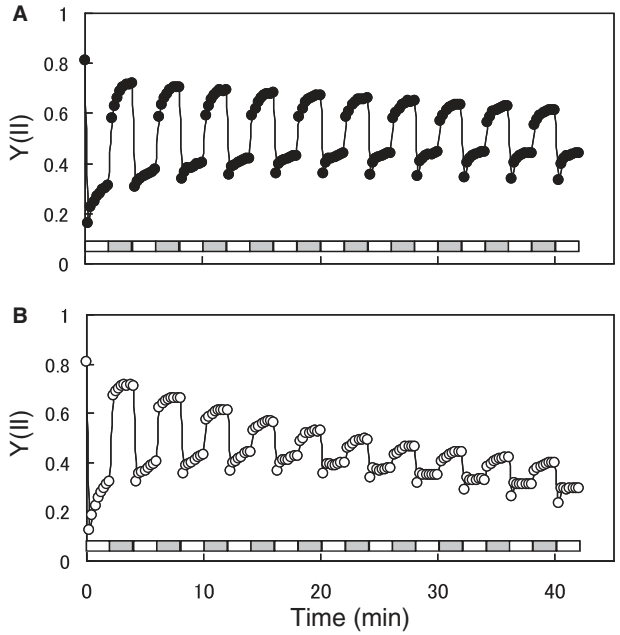

Fig. 1 Response of the photochemical quantum yield of PSII [Y(II)] of the WT (A) and *pgr5* (B) plants to the fluctuating light. The plants were grown in a constant moderate light (100 μmol photons $m^{-2}s^{-1}$) for 8 h d^{-1}. The light alternating between HL at 240 μmol photons $m^{-2}s^{-1}$ for 2 min (open bars) and LL at 30 μmol photons $m^{-2}s^{-1}$ for 2 min (grey bars) was applied to the leaf after the dark treatment for 30 min. The leaf lamina was sandwiched in a chamber. The air in the chamber contained 20% O_2 and 390 p.p.m. CO_2. Each data point represents the mean ($n = 5–6$).

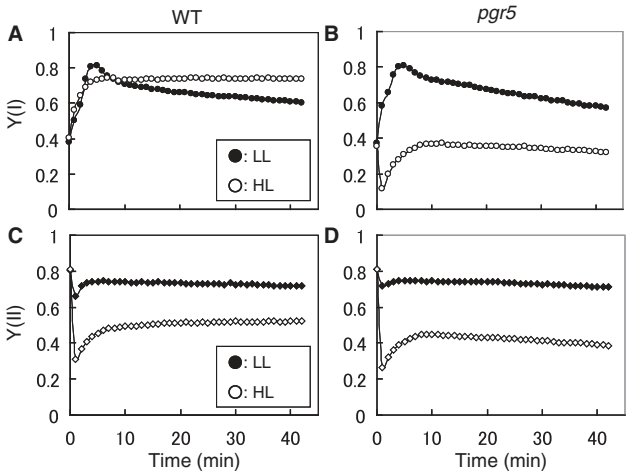

Fig. 2 Changes in the quantum yield of PSI [Y(I)] and PSII [Y(II)]. (A and B), Y(I); (C and D), Y(II). Constant light at a PPFD of 240 μmol photons $m^{-2}s^{-1}$ (open symbols, HL) or at a PPFD of 30 μmol photons $m^{-2}s^{-1}$ (filled symbols, LL) was applied for 42 min after the 30 min dark treatment. Measurements were made at 20% O_2 and 390 p.p.m. CO_2. Each data point represents the mean ($n = 4$).

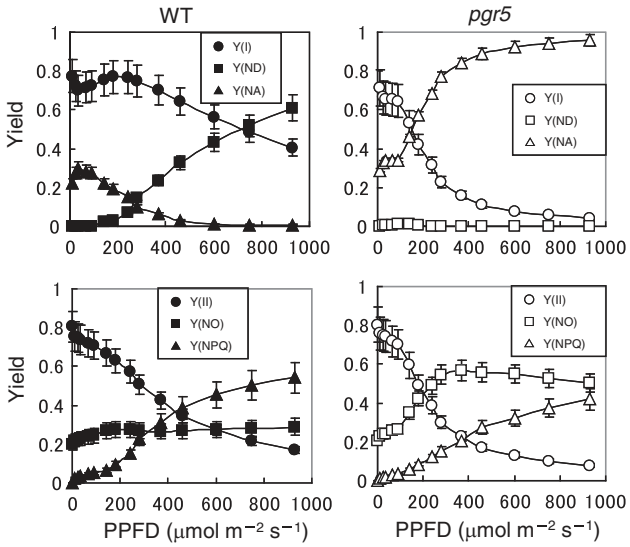

Fig. 3 Changes in the photosynthetic quantum yields of PSI and PSII with the PPFD of constant light in the WT (filled symbols) and *pgr5* (open symbols). For energy captured by PSI pigments, the quantum yield of the PSI photochemistry, Y(I) (circle), the quantum yield of non-photochemical energy dissipation due to the donor-side limitation, Y(ND) (square), and that of the energy dissipation due to the acceptor-side limitation, Y(NA) (triangle), are indicated. The fluorescence parameters, the effective PSII quantum yield, Y(II) (circle), the quantum yield of regulated energy dissipation, Y(NPQ) (triangle), and that of non-regulated energy dissipation, Y(NO) (square) are shown. Measurements were made at 20% O_2 and 390 p.p.m. CO_2. The values represent the mean ± SD ($n = 4–6$).

To compare the photosynthetic responses in fluctuating light and those in continuous light, we measured changes in Y(II) and the PSI quantum yield, Y(I), in constant HL at 240 μmol photons $m^{-2}s^{-1}$ or LL at 30 μmol photos $m^{-2}s^{-1}$ for 42 min (**Fig. 2**). When the plants that had been kept in the dark for >30 min were exposed to the constant HL, Y(I) of the WT increased for about 5 min and attained a steady level, while that in LL gradually decreased. Y(II) in HL once decreased, attained a steady level, while that in LL decreased and attained the peak value at around 5 min and then slightly decreased. In the *pgr5* plants, Y(I) in LL showed a transient similar to that of the WT. Y(I) in HL, however, once decreased, increased to the peak at around 10 min and then decreased very slightly. Changes in Y(II) in *pgr5* were similar to those in the WT. In HL, both Y(I) and Y(II) in *pgr5* were considerably lower than those in the WT.

Light responses of the steady-state PSI and PSII parameters at various PPFDs

Light responses of PSI and PSII parameters obtained from Chl fluorescence and P700 signals were further analyzed (**Fig. 3**). For energy captured by PSI pigments, the quantum yield of the PSI photochemistry, Y(I), the quantum yield of non-photochemical energy dissipation due to the donor-side limitation, Y(ND), and that of the energy dissipation due to the acceptor-side limitation, Y(NA), were measured. The fluorescence parameters measured included the effective PSII quantum yield, Y(II), the quantum yield of regulated energy dissipation, Y(NPQ), and that of non-regulated energy dissipation, Y(NO).

Y(I) and Y(II) in both the WT and *pgr5* decreased with the increase in PPFD. In the WT, Y(NA) was greater than Y(ND) at PPFDs <250 μmol photons $m^{-2} s^{-1}$, while, above this level, Y(NA) decreased and Y(ND) increased. In the WT, with the increase in PPFD, Y(NPQ) markedly increased, while Y(NO) increased only slightly. *pgr5* showed trends very different from those of the WT. Y(NA) of *pgr5* was similar to that of the WT up to 100 μmol photons $m^{-2} s^{-1}$, but it markedly increased with further increases in PPFD, causing a drastic decrease in Y(I) in *pgr5* at PPFDs >150 μmol photons $m^{-2} s^{-1}$. Y(ND) in *pgr5* was nearly zero over the entire PPFD range. These results indicate that, at high PPFDs, the electron flow through PSI in *pgr5* was limited by the acceptor-side reactions. Furthermore, the increase in Y(NPQ) was much less than that in the WT, while Y(NO) markedly increased.

Effects of fluctuating light on photoinhibition of photosystems and photosynthetic electron transport

The maximum level of the P700 signal (full oxidation of P700) in the dark (ΔA_{max}) and the maximum quantum yield of PSII (F_v/F_m) were measured before and after the treatment with constant HL (240 μmol photons $m^{-2} s^{-1}$) or fluctuating light (alternating between HL at 240 μmol photons $m^{-2} s^{-1}$ for 2 min and LL at 30 μmol photons $m^{-2} s^{-1}$ for 2 min), both for 42 min (**Fig. 4**). After the light treatments, plants were kept in the dark for 30 min and ΔA_{max} and F_v/F_m were measured. ΔA_{max} and F_v/F_m were unchanged after the constant HL treatment for 42 min from the levels before the treatment (**Fig. 4a, c**), indicating that photoinhibition of photosystems hardly occurred. Y(NA) and 1 – qL were measured in LL at 30 μmol photons $m^{-2} s^{-1}$ for 5 min before and after the 42 min light treatment. The data obtained at the end of 5 min of LL are denoted as $Y(NA)_{30}$ and $1 - qL_{30}$, respectively. After the HL treatment, both $Y(NA)_{30}$ and $1 - qL_{30}$ in *pgr5* were significantly higher than before (**Fig. 4b, d**), indicating some damage to the acceptor side of PSI.

The WT showed small decreases both in ΔA_{max} and in F_v/F_m after the treatment with the fluctuating light treatment (**Fig. 4e, g**). In contrast, ΔA_{max} in the *pgr5* plants after the fluctuating light treatment decreased by 38%, while F_v/F_m decreased only slightly. Although there were only small decreases in ΔA_{max} and F_v/F_m in the WT, $Y(NA)_{30}$ and $1 - qL_{30}$ after the fluctuating light treatment increased by 42% and 135% (**Fig. 4f, h**), respectively, indicating some damage to the acceptor side of PSI and the competence of PSI in oxidizing the intersystem chain. In *pgr5*, $Y(NA)_{30}$ and $1 - qL_{30}$ increased by 94% and 332% after the fluctuating light treatment.

Do the *pgr5* plants show CEF-PSI activity in constant light?

To investigate whether the *pgr5* plants showed CEF-PSI activity in constant light, we estimated the ETR through PSI [ETR(I)] and PSII [ETR(II)] simultaneously. The photochemical quantum yield of PSI, Y(I), may be expressed as $Y(I) = Y(L_I) + Y(WWC) + Y(CEF_I)$, where $Y(L_I)$, Y(WWC) and $Y(CEF_I)$ are the quantum yields of the LEF through PSI, the WWC and the CEF-PSI, respectively. Similarly, the photochemical quantum yield of PSII, Y(II), may be written as

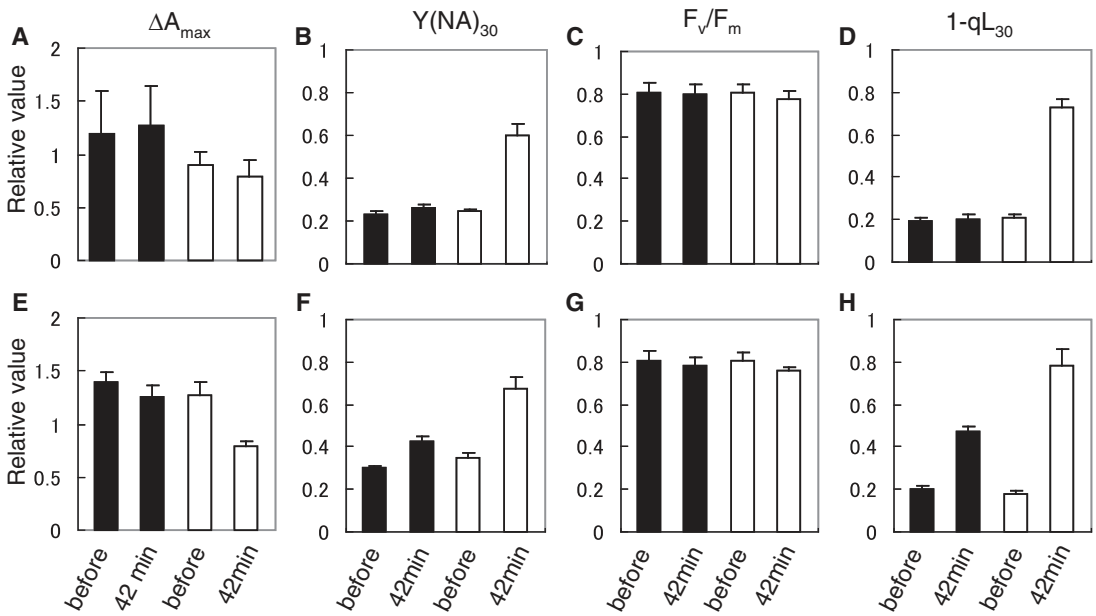

Fig. 4 Effects of constant high light (a–d) and fluctuating light (e–h) on changes in photosynthetic parameters in leaves of the WT (filled bars) and *pgr5* (open bars). Following the light treatments for 42 min and dark treatment for 30 min, the functions of the PSI and PSII reaction centers were determined as ΔA_{max} and F_v/F_m. $Y(NA)_{30}$ and $1 - qL_{30}$ were measured at the end of the low light treatment at a PPFD of 30 μmol photons $m^{-2} s^{-1}$ for 2 min just after the light treatments for 42 min. Measurements were made at 20% O_2 and 390 p.p.m. CO_2. Error bars represent the SD ($n = 6–8$).

$Y(II) = Y(L_{II}) + Y(WWC)$, where $Y(L_{II})$ is the quantum yield of the LEF through PSII.

To obtain directly comparable ETR(I) and ETR(II) values, we measured leaf absorptance, and estimated the share of absorbed light energy allocated to PSII (f_{PSII}). **Fig. 5A** shows the relationships between the gross O_2 evolution in the air containing 5% CO_2 and the absorbed PPFD at low PPFDs calculated with the absorptance values, measured in four leaves each of the WT and *pgr5*, respectively. When compared at the same absorbed PPFD, the O_2 evolution rates for *pgr5* leaves was always lower than that for the WT leaves, indicating that the quantum yield of O_2 evolution on the absorbed quantum basis was lower in the *pgr5* leaves. However, F_v/F_m values in the leaves did not differ between the WT and *pgr5*. **Fig. 5B** shows relationships between the quantum yield of gross O_2 evolution [$Y(O_2)$] and that of PSII photochemistry [Y(II)] in the same leaves used for **Fig. 5A**. The slope of the line should be proportional to the share of absorbed light energy allocated to PSII (f_{PSII}). In *pgr5*, the slope was lower by 17.3% than in the WT. The share of absorbed light energy allocated to PSII was 35 ± 3.4% in *pgr5*, while the share in the WT was 47 ± 4.1%. With these values, it would be possible to calculate the absolute rates of ETR(I) and ETR(II).

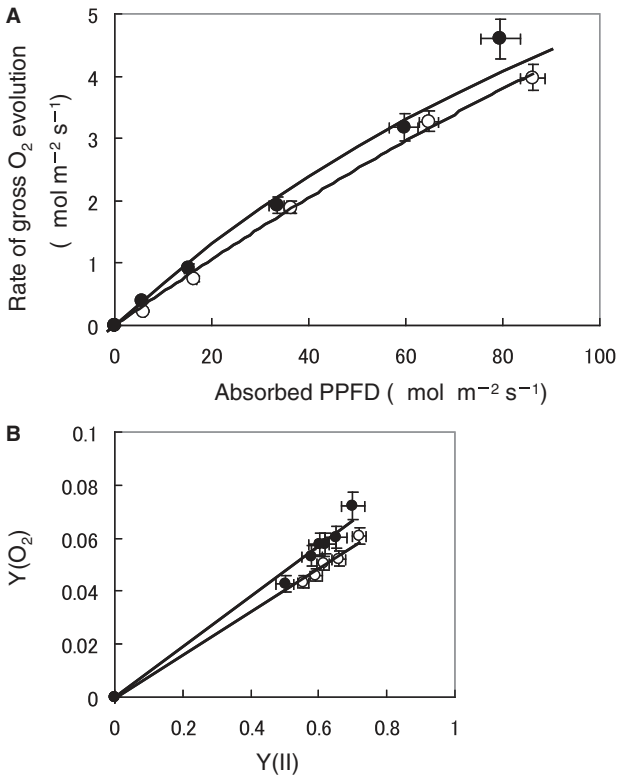

Fig. 5 Estimation of the share of absorbed light energy to PSII. (A) Light–response curve of the photosynthetic O_2 evolution in the leaf disks at low PPFDs. The rate of gross O_2 evolution was plotted against absorbed PPFD, Fitted hyperbolic functions through the origin are shown. (B) The relationship between the quantum yield of O_2 evolution, $Y(O_2)$, and the photochemical yield of PSII, Y(II). Filled circle, WT; open circle, *pgr5*. Error bars represent the SD ($n = 4–6$). Regression lines through the origin are shown.

In the WT plants, the ETR(I)/ETR(II) ratio was close to 1 at PPFDs below 100 μmol photons $m^{-2} s^{-1}$, and subsequently increased with the increase in PPFD. In contrast, the ETR(I)/ETR(II) ratio in *pgr5* was high at low PPFDs and decreased with the increase in PPFD, and eventually became close to 1 (**Fig. 6**). In accordance with the widely accepted view, the contribution of the CEF-PSI increased with the increase in PPFD in the WT, while *pgr5* showed a contrasting trend: the contribution of CEF-PSI decreased with the increase in PPFD.

The ETR(I)/ETR(II) ratio would not be correct if there were large changes in the energy share between PSII and PSI due to the state transition. To examine the contribution of the state transition to the change in the ETR(I)/ETR(II) ratio, we determined the components of non-photochemical Chl fluorescence quenching, qN, from the relaxation kinetics of qN in the dark. **Fig. 7** shows the extents of qE, state transition quenching (qT) and photoinihibitory quenching (qI) after 20 min of constant light at PPFDs of 30, 240 and 470 μmol photons $m^{-2} s^{-1}$. Both WT and *pgr5* leaves exhibited substantial qE, although qE in the *pgr5* leaf was much less than that in WT plants, as was reported previously (Munekage et al. 2002, Munekage et al. 2008). qT components were small compared with qE in both plants. As the measurements were carried out with red actinic light, there was no effect of chloroplast avoidance movement on the apparent state transition (Cazzaniga et al. 2013). Therefore, it is unlikely that the state transition affected the ETR(I)/ETR(II) ratio very much.

Table 1 shows the Chl contents on a leaf area basis in WT and *pgr5* leaves. The Chl content was higher in the WT than in *pgr5*. There were some differences in absorptance, reflecting the difference in the Chl content. The Chl *a*/*b* ratio in the *pgr5* leaves was greater than that in WT leaves by 0.4.

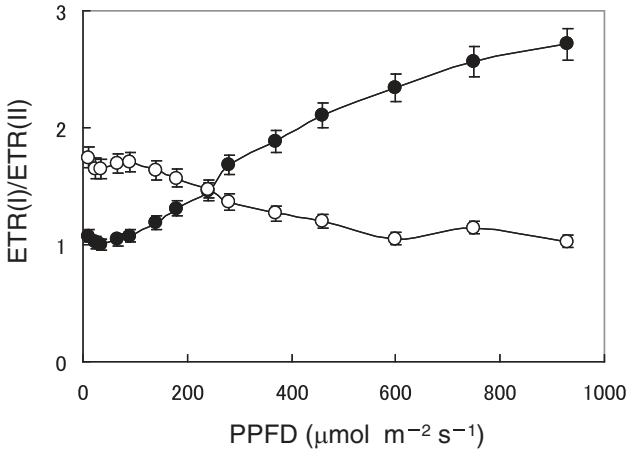

Fig. 6 Changes in the ETR(I)/ETR(II) ratio in WT (filled circle) and *pgr5* (open circle) leaves as a function of the PPFD of constant light. Y(I) and Y(II) were measured as in **Fig. 3**. Measurements were made at 20% O_2 and 390 p.p.m. CO_2. The values represent the mean ± SD ($n = 4–6$).

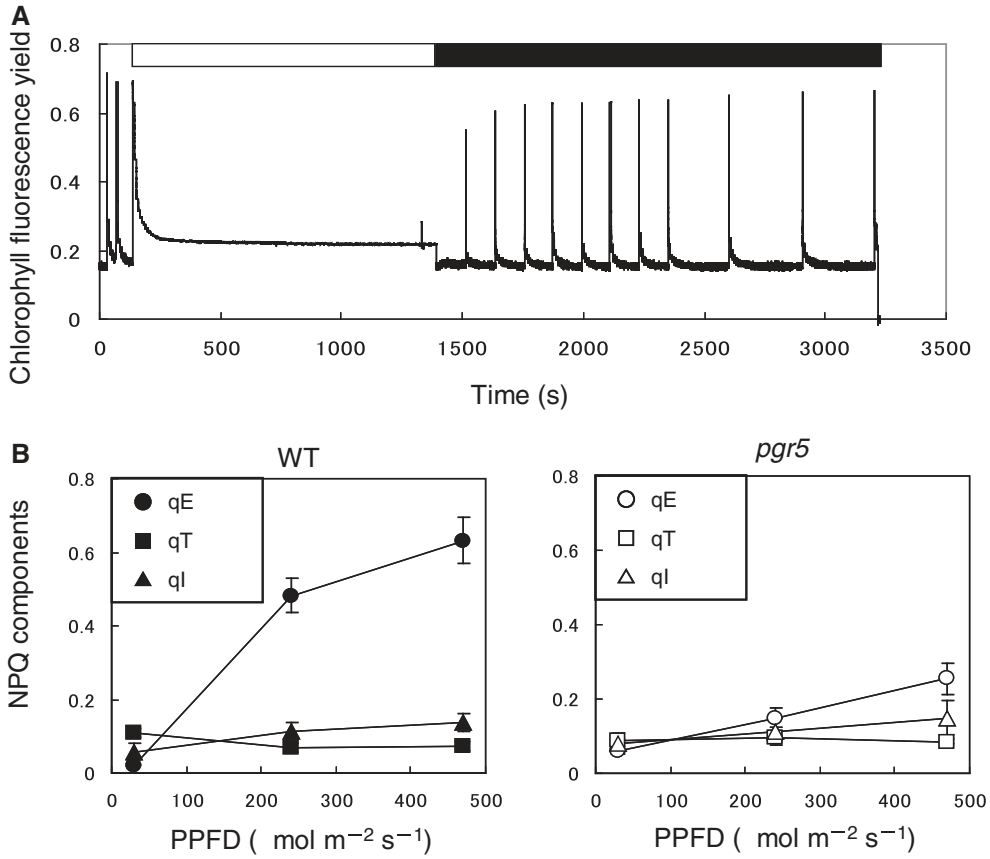

Fig. 7 Dissection of the non-photochemical quenching into energy-dependent quenching (qE), state transition quenching (qT) and photoinhibition quenching (qI). (A) A typical Chl fluorescence trace obtained with a WT leaf after 30 min dark adaptation. The trace shows the changes in fluorescence yield during (white bar) and after turning off the actinic light (black bar). (B) Components of non-photochemical Chl fluorescence quenching in the WT and *pgr5*. The different components of non-photochemical fluorescence quenching were derived from semi-logarithmic plots of the dark relaxation of F_v after the light treatment at three PPFDs of 30, 240 and 470 μmol photons $m^{-2}s^{-1}$. Energy-dependent quenching (qE; circle) was attributed to the fast phase, quenching by state transition (qT; square) to the medium phase and photoinhibitory quenching (qI; triangle) to the slow phase of relaxation. The quenching components were calculated from the amplitude of the respective phases considering the relationship $(1 - qN) = (1 - qE) \times (1 - qT) \times (1 - qI)$. Measurements were made at 20% O_2 and 390 p.p.m. CO_2. The values represent the mean ± SD ($n = 3$).

Table 1 Chl $a + b$, Chl a/b in thylakoids and leaf absorptance in the WT and *pgr5* leaves

Genotype	Chl $a + b$ (mg m^{-2})	Chl a/b	Leaf absorptance
WT	228 ± 23	3.38 ± 0.007	0.837 ± 0.0521
pgr5	190 ± 10*	3.73 ± 0.009*	0.823 ± 0.0742*

Plants were grown at 90–100 μmol $m^{-2}s^{-1}$ in a short-day photoperiod (8 h of light, 16 h of dark) for 55 d.
Means ± SD ($n = 3$–5) are shown.
Light absorptance was measured with an integrating sphere. The light from the Björkman-type lamp passing through a 635 nm red filter was used.
*$P < 0.005$ (*t*-test, WT vs. *pgr5*).

Does the WWC in the *pgr5* plants function in constant light?

Next, we investigated whether the *pgr5* plants were able to drive the WWC. In the WWC, the electron acceptor from PSI is O_2 and the extent of the electron flow to the WWC depends on the O_2 concentration (Miyake and Yokota 2000). The CEF-PSI activity has been shown to increase at a low O_2 concentration, indicating suppression of the WWC by low O_2 (Arnon and Chain 1975, Arnon and Chain 1979, Scheller 1996, Makino et al. 2002). If the *pgr5* plants possessed no WWC capacity, the activity of the CEF-PSI would not be enhanced even at low O_2 concentrations. We measured the light dependence of the ETR(I)/ETR(II) ratio on the O_2 concentration in the chamber, namely at 20, 2.7 and 0% O_2 (**Fig. 8**). In the *pgr5* plants, the ETR(I)/ETR(II) ratios at 2.7% and 0% O_2 were higher than that at 20% O_2 when the PPFD was >100 μmol photons $m^{-2}s^{-1}$. Both the WT and *pgr5* exhibited the highest ETR(I)/ETR(II) ratios at 2.7% O_2 at any PPFD below 300 μmol photons $m^{-2}s^{-1}$. Therefore, it is likely that the *pgr5* plants possessed the capacity for the WWC.

Response of the ETR(I)/ETR(II) ratio to fluctuating light

Changes in the ETR(I)/ETR(II) ratio in fluctuating light are shown in **Fig. 9**. The same fluctuating light regime as used for the data in

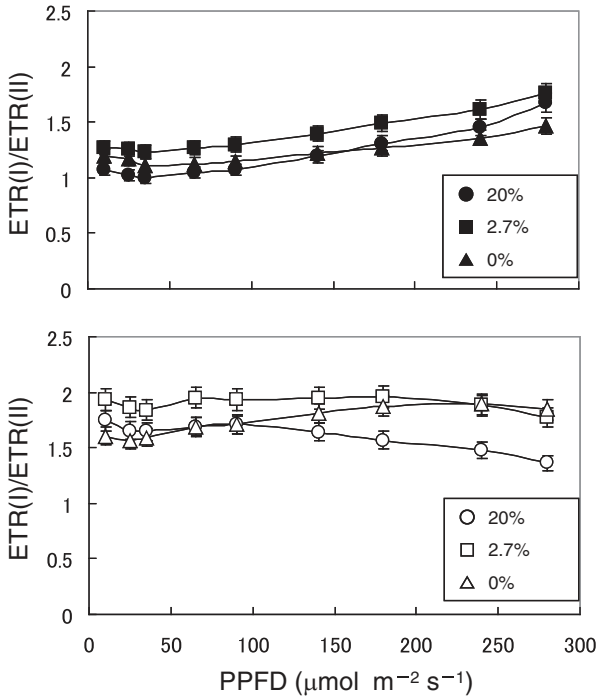

Fig. 8 Light intensity dependence of the ETR(I)/ETR(II) ratio in 20, 2.7 and 0% O_2 in WT (filled symbols) and *pgr5* (open symbols) leaves. Measurements were made for the PPFDs ranging from 0 to 280 μmol photons $m^{-2} s^{-1}$ and at a CO_2 concentration of 390 p.p.m. The values represent the mean ± SD ($n = 3$).

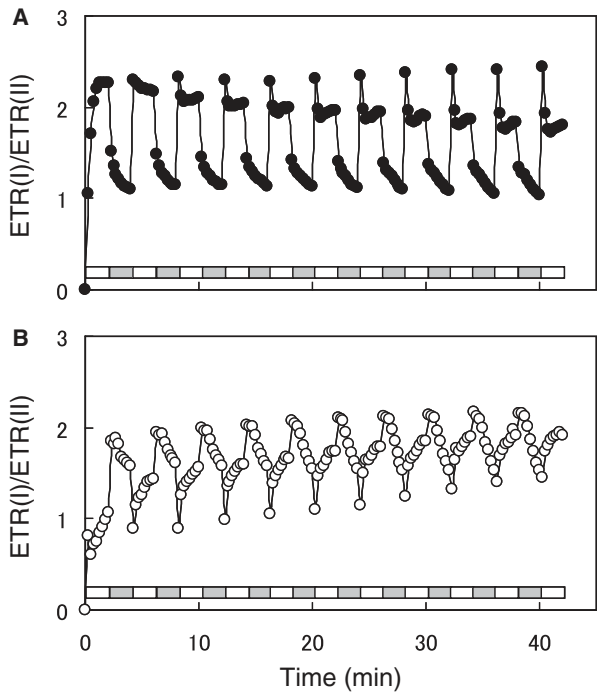

Fig. 9 Changes in the ETR(I)/ETR(II) ratio in WT (A) and *pgr5* (B) leaves in fluctuating light. The same light treatment protocol as in **Fig. 1** was used. Measurements were made at 20% O_2 and 390 p.p.m. CO_2. The values represent the mean ± SD ($n = 5–6$).

Fig. 1 was used. Consistent with the data in **Fig. 6**, the ETR(I)/ETR(II) ratio in the *pgr5* plants was lower in the HL period than in the LL period, whereas WT plants showed a higher ETR(I)/ETR(II) ratio in the HL period than in the LL period. In the WT, the ETR(I)/ETR(II) ratio reached a maximum at 15 s after each transfer from the LL period to the HL period, and, within 2 min, decreased slowly toward the steady-state value. The maximal value at 15 s after the transfer gradually increased with the cycle, while the steady-state value slightly decreased. In contrast, in *pgr5*, the ETR(I)/ETR(II) ratio rapidly decreased to the minimum at 15 s after the transfer from the LL period to the HL period. The minimal value gradually increased with the cycles. Also the ratio at the last data point in the HL period increased with the cycle. The peak value in the 2 min LL period gradually increased. In each of the LL periods, the ratio decreased.

Effects of O_2 concentration on responses of electron transport to fluctuating light

Responses of Y(II) to the fluctuating light were measured at 2.7% and 0% O_2 (**Fig. 10**). In *pgr5*, Y(II) at the end of the LL period decreased only slightly with the cycle at 2.7% O_2. The decrease in Y(II) in LL was smaller still at 0% O_2. Moreover, in contrast to the gradual decrease in Y(II) in the HL period at 20% O_2, Y(II) in HL increased with the cycle at 2.7% and 0% O_2. Similarly, in the WT, Y(II) at the end of the LL period did not decrease with the cycle at 2.7% or 0% O_2, whereas Y(II) at the end of the LL period decreased at 20% O_2. Y(II) in the HL period

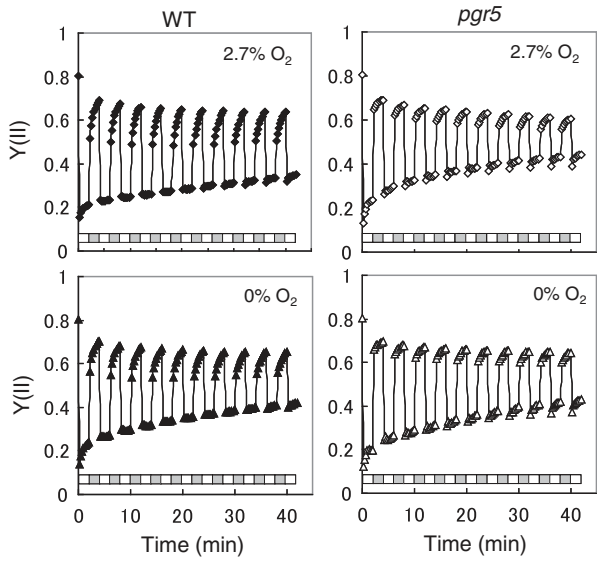

Fig. 10 Effects of low O_2 concentrations (2.7%, diamond; 0%, triangle) on responses of Y(II) to the fluctuating light in the WT (fillsed symbol) and *pgr5* (open symbol). The fluctuating light treatment was the same as that used for **Fig. 1**. Measurements were made at 390 p.p.m. CO_2. The values represent the mean ($n = 4–6$).

at 2.7% and 0% O_2 continued to increase with the cycle and did not reach the steady-state values within 42 min.

We assessed the degrees of photoinhibition after the treatment with fluctuating light for 42 min at 0, 2.7 or 20% O_2 and

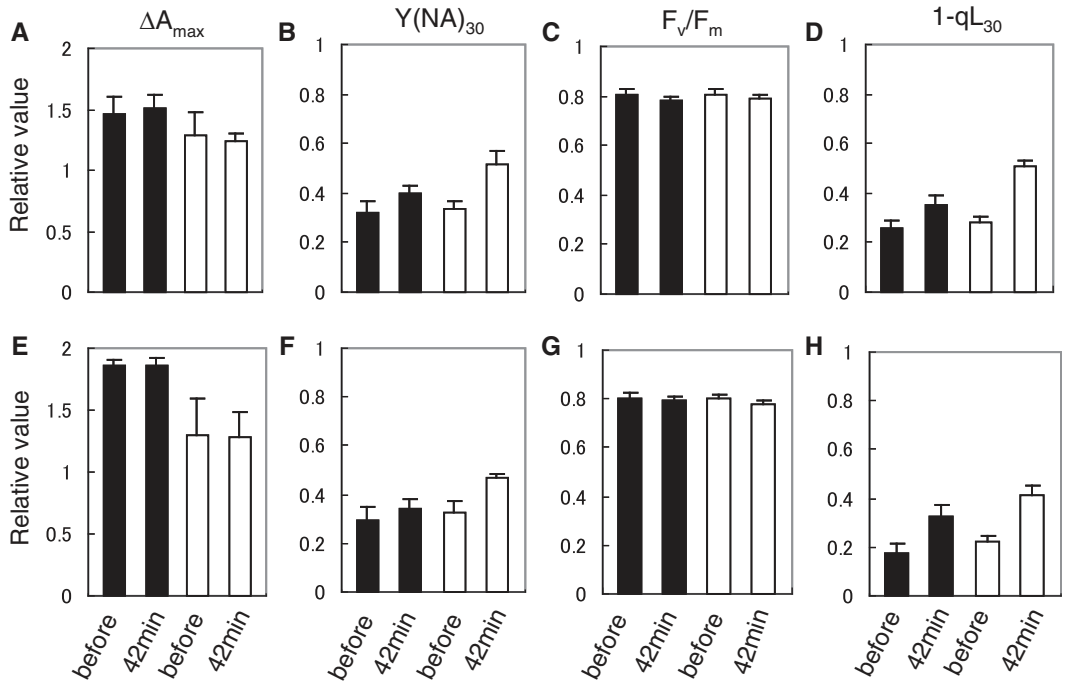

Fig. 11 Effects of low O_2 concentrations (2.7%, a–d; 0%, e–h) on changes in photosynthetic parameters after the fluctuating light treatment in the WT (black bar) and *pgr5* (white bar). Measurements were made in the same manner as in **Fig. 4** and at 390 p.p.m. CO_2. Error bars represent the SD ($n = 4–8$).

dark treatment for 30 min (**Fig. 11**) using the same experimental protocol that was used for the data shown in **Fig. 4**. The *pgr5* plants showed little photoinhibition of PSI at 2.7% and 0% O_2 compared with that at 20% O_2 (cf. **Fig. 4e** and **Fig. 11a** and **e**). The marked increases observed in $Y(NA)_{30}$ and $1 - qL_{30}$ after the light treatment at 20% O_2 were greatly suppressed at low O_2, although the increases were consistently observed not only in *pgr5* but also in the WT.

Discussion

Fluctuating light as a stress factor causing photodamage

How plants use sunflecks—pulses of light at high intensity—is a topic that has attracted the attention of researchers for decades (Allee 1926, Evans 1956). There have been many laboratory-based mechanistic studies as well as field-oriented studies focusing on photosynthetic responses to fluctuating light. For instance, photosynthetic responses of plants grown in controlled fluctuating light and those grown in constant light were compared (Yin and Johnson 2000, Alter et al. 2012, Suorsa et al. 2012). The responses were also compared between plants grown in natural fluctuating light in a forest understorey and those grown in an open field site (Knapp and Smith 1989). In most of these studies, photosynthetic responses to a single light pulse were examined. However, in natural environments, such as the forest understorey, light fluctuates more frequently, as many researchers quantified (Pearcy 1983, Chazdon 1988, Vierling and Wessman 2000). Although there have been some pioneering studies (Alter et al. 2012, Suorsa et al. 2012), our knowledge of the photosynthetic responses to fluctuating light is still poor.

It is important to choose appropriate fluctuating light regimes for studying plant responses to fluctuating light. The light environment in the forest understorey changes drastically due to sunflecks. Most sunsflecks are less than several minutes in length, and have a PPFD more than several-fold that of LL periods (Pearcy 1983, Koizumi and Oshima 1993, Vierling and Wessman 2000). Recently, Suorsa et al. (2012) grew several mutant lines of *A. thaliana* in the light alternately changing from LL at 50 μmol photons $m^{-2}s^{-1}$ for 5 min to high HL at 500 μmol photons $m^{-2}s^{-1}$ for 1 min, and successfully elucidated a role for the PGR5 protein in acclimation to the fluctuating light. In the present study, we used a fluctuating light regime with the same durations of HL and LL. The duration we adopted was 2 min because the photosynthetic parameters change most drastically upon the change from the LL to the HL period in the first 2 min in *A. thaliana* plants. Thus, the light fluctuation in the 2 min intervals would subject the plants to the most stressful situation. Next, we chose the intensity of the HL. The HL at 240 μmol photons $m^{-2}s^{-1}$ was strong enough, but did not induce photoinhibition when given continuously. The present results indicate that the fluctuating light we adopted was suitable for analysis of the effects of fluctuating light on photoinhibition. The results clearly showed that light fluctuation itself is a very effective stress factor causing photodamage. We propose the term 'fluctuating light photoinhibition' and the target is mainly PSI, as has been

already indicated by pioneering studies (Munekage et al. 2002, Munekage et al. 2008, Suorsa et al. 2012).

Effects of short-term fluctuating light on the photosynthetic electron transport system

The decreases in the photochemical quantum yield of PSII, Y(II), of the WT and *pgr5* plants occurred soon after the start of the fluctuating light treatment. Y(II) of *pgr5* decreased more drastically (**Fig. 1**). Moreover, these plants showed photoinhibition of PSI by the fluctuating light treatment. In particular, the extent of PSI photoinhibition in *pgr5* was marked. It should be noted that this was not the result of the long-term effect of the fluctuating 'growth' light (Suorsa et al. 2012) but that of treatment for a short period. It has been reported that PSI of *pgr5* was sensitive to light (Munekage et al. 2002, Munekage et al. 2008). In the present study, we found that PSI activity in *pgr5* was limited by the acceptor-side reactions: Y(NA) was higher than Y(ND) over the entire PPFD range examined (**Fig. 3**).

What component/event in the PSI acceptor side limited the photochemical reaction and thereby caused PSI photoinhibition? The crucial difference between the fluctuating light and constant light was that fluctuating light included a LL period, during which photosynthetic activities were lower than those during the HL period. When leaves were in the LL, various reactions that had occurred in response to HL, including the de-epoxidation of violaxanthin and protonation of the PsbS protein, would be relaxed to some extent. In the HL period, the thylakoid lumen acidification would not be enough for down-regulation of LEF via the photosynthetic control of plastoquinol re-oxidation at the Cyt b_6/f complex (Rott et al. 2011, Suorsa et al. 2012), particularly in *pgr5*. Therefore, especially in *pgr5*, when every HL period started, the thylakoids in the more or less relaxed state would cause a gush of electron flow to PSI, leading to prompt reduction of electron acceptors, O_2 photoreduction and formation of ROS. From preceding studies (Sonoike 1996, Sonoike et al. 1997, Choi et al. 2002), it is clear that the photoinhibition of PSI involves ROS and thereby requires O_2.

It is noteworthy that the PSI photoihibition occurred even in the WT plants due to the fluctuating light; the photodamage by fluctuating light is not a phenomenon specific only to *pgr5*.

The response to fluctuating light effectively avoiding photoinhibition

The large Y(NA) means a high level of PSI acceptor-side limitation. This is not necessarily directly associated with photoinhibition of PSI. As clearly shown in **Fig. 4**, *pgr5* treated in continuous HL showed little photoinhibition of PSI, although $Y(NA)_{30}$ and $1 - qL_{30}$, measured at the end of the illumination of 30 μmol photons $m^{-2} s^{-1}$ for 2 min, just after the constant HL for 42 min, were very high. On the other hand, when fluctuating light was applied for 42 min, PSI photoinhibition occurred in both the WT and *pgr5*, in addition to the increases in $Y(NA)_{30}$ and $1 - qL_{30}$. The extent of the damage was markedly greater in *pgr5*. The large difference in the PSI photoinhibition between the WT and *pgr5* plants indicates that the WT had mechanisms to cope with rapid light fluctuations. We hypothesized that this would be related to photosynthetic alternative electron flows interacting with PSI because PSI was first photoinhibited in the fluctuating light. Previous studies reported that, in *pgr5*, the CEF-PSI via the putative FQR was impaired (Munekage et al. 2002, Munekage et al. 2004, DalCorso et al. 2008). However, some other studies reported that *pgr5* possessed CEF-PSI capacity (Nandha et al. 2007, Joliot and Johnson 2011). We tried to assess the activities of the alternative electron flows in *pgr5*.

Several methods have been used to quantify the rate of the CEF-PSI (for a review, see Kramer et al. 2004a). In LEF, the rates of electron transfer through PSII should equal that through PSI (Klughammer and Schreiber 1994) or the Cyt b_6/f complex (Klughammer and Schreiber 1994, Sacksteder and Kramer 2000). Thus, the relationship between some factors associated with the electron flow and the LEF should be changed when the activity of the CEF-PSI becomes substantial. In turn, from the increased ratios of these factors to LEF, the rate of the CEF-PSI would be assessed. The possible factors would include the proton to electron stoichiometry (Sacksteder et al. 2000), electrochromic shift of carotenoid pigments due to the formation of an electric field across the thylakoid membrane (Joliot and Joliot 2002, Joliot and Joliot 2005, Joliot et al. 2004, Sacksteder and Kramer 2000) and the proportion of overall photosynthetic energy storage assessed by the photoacoustic method (Herbert et al. 1990, Joet et al. 2002). More directly, measurements of post-illumination re-reduction kinetics of $P700^+$ after red + far-red actinic light (Fan et al. 2007), or after a far-red illumination (Maxwell and Biggins 1976, Joet et al. 2002, Chow and Hope 2004), have been conducted. The transient rise in the fluorescence level after turning off the actinic light has also been measured as a parameter reflecting the activity of CEF-PSI (Asada et al. 1993, Burrows et al. 1998). However, it is not feasible to measure the absolute rate of the CEF-PSI in situ with these techniques. Instead, we used the ETR(I)/ETR(II) ratio as an indicator of the CEF-PSI activity (**Fig. 6**). Because the linear electron transport rate through PSII can be quantified (Genty et al. 1989), if the ratio is properly obtained, the rate through PSI may be quantified. For this purpose, we measured leaf absorptance and the share of absorbed light energy allocated to PSII (f_{PSII}) (**Table 1**). Very recently, Kou et al. (2013) estimated the activity of PSI-CEF at saturating CO_2 based on measurements of the O_2 evolution rate and PSI quantum yields. However, they did not measure f_{PSII}.

Solving the equation, $Y(O_2) = I_A \times f_{PSII} \times Y(II)/4$, where I_A is the absorbed PPFD (Genty et al. 1989), we obtained the share of absorbed light energy allocated to PSII. In spite of the fact that the plants were grown under constant illumination, the share in *pgr5* was 35%, while the WT showed almost equal sharing of light energy between PSI and PSII (**Fig. 5B**). Furthermore, the contribution of the state transition to the energy share was small over the range from low to high PPFD in both plants (**Fig. 7**), in agreement with the studies reporting that the state transitions

in higher plants were not marked (Pesaresi et al. 2011). These results indicate that the share of light energy allocation to PSI was much greater than that to PSII in *pgr5*. In the light–response curve shown in **Fig. 3**, Y(I) in *pgr5* started to decrease from very low PPFDs, whereas that in the WT was relatively high up to a PPFD of approximately 250 μmol photons $m^{-2}s^{-1}$ and started to decrease with a further increase in PPFD. In *pgr5*, a limitation of electron flow through PSI due to this decrease in Y(I) at low PPFD would be compensated by the increase in the share of absorbed light energy allocated to PSI. This was also supported by the fact that the Chl *a*/*b* ratio was greater in the *pgr5* leaves than that in the WT by 0.4. Previous studies reported that growth of *pgr5* was similar to that of the WT in both low light (Munekage et al. 2008) and moderate light (Suorsa et al. 2012). However, in fact, energy sharing between the two photosystems and the composition of Chl proteins would be markedly changed in *pgr5*. The calculation of the ETR using properly measured f_{PSII} may be a useful method to estimate CEF-PSI.

When white light was used for the actinic light, maximum $Y(O_2)$ values for non-stressed leaves of C_3 plants approached 0.105 (Björkman and Demmig 1987). In this study, $Y(O_2)$ decreased with the absorbed PPFD at low PPFDs because red light was used for the actinic light. However, when the maximum $Y(O_2)$ was obtained by extrapolating the line in **Fig. 5B** to a Y(II) of 0.81, the value for the WT was 0.09, a value within the range of the data for C_3 species (Björkman and Demmig 1987).

From the light energy allocation to PSI and the changes in the ETR(I)/ETR(II) ratio measured in the constant and fluctuating light, we suggest that *pgr5* plants possessed CEF-PSI activities because the ratios at low PPFDs and LL in the fluctuating light were far greater than 1 (**Figs. 6**, **9**). These results also indicate that, under the growth light conditions at a PPFD of 100 μmol photons $m^{-2}s^{-1}$, *pgr5* drove CEF-PSI continuously (Nandha et al. 2007). On the other hand, the ETR(I)/ETR(II) ratio in the WT increased with the increase in PPFD. This suggests that the CEF-PSI functions not only during photosynthetic induction (Makino et al. 2002, Joliot and Joliot 2002, Joliot and Joliot 2005, Joliot and Joliot 2006, Fan et al. 2007) but also under steady-state conditions in high light.

There are some O_2-dependent pathways besides the WWC, and they may contribute to the photodamage by the fluctuating light. Photorespiration is one of the O_2-dependent pathways. When CO_2 and O_2 concentrations were 800 p.p.m. and 20%, respectively, in the leaf chamber where the effect of photorespiration was suppressed to a considerable extent, Y(II) of the WT and *pgr5* showed responses similar to those at 390 p.p.m. and 20% (**Supplementary Fig. S1**). Plastid terminal oxidase (PTOX) is also proposed to be associated with O_2 consumption, in the reaction called chlororespiration. The PTOX is a plastoquinol oxidase, and is able to transfer electrons from PQ to O_2. Thus, chlororespiration can be a source of ROS generation. However, PTOX is suggested to play an important role in chloroplast biogenesis rather than in stress responses (Rosso et al. 2006). Furthermore, in plants grown under normal conditions, PTOX is present at about only 1% of the level of the D1 protein that houses the PSII reaction center (Lennon et al. 2003). Therefore, the contributions of photorespiration and chlororespiration to the photodamage caused by the fluctuating light would be small, if any.

In both the constant and fluctuating light, *pgr5* appeared to show WWC activities (**Fig. 8**). When the light dependence of the ETR(I)/ETR(II) ratio was measured at 2.7% or 0% O_2, the ratios in *pgr5* at a PPFD >100 μmol photons $m^{-2}s^{-1}$ were greater than those measured at 20% O_2. This suggests that at least some fraction of electrons that flowed through the WWC at 20% O_2 would flow through the CEF-PSI at low O_2 concentrations, resulting in increases in the ETR(I)/ETR(II) ratio. The ETR(I)/ETR(II) ratios in the WT and *pgr5* were highest at 2.7% O_2 rather than at 0% O_2 for all the PPFD levels examined (**Fig. 8**). The reasons for this are unknown.

For WT plants in the fluctuating light, the ETR(I)/ETR(II) ratio in the HL periods rapidly increased immediately after each transition from the LL to the HL period, attained maximal levels, then decreased and attained steady-state values within the HL periods. Although the steady-state values decreased in a stepwise fashion with the cycle, the maximal levels were almost constant. In contrast, in *pgr5*, the ratio rapidly decreased immediately after each transition from an LL to a HL period and then attained the minimum levels within the HL periods. Under these conditions, PSI of *pgr5* would be more sensitive to the damage due to the fact that PSI capacity was not able to manage the gush of electron flow caused by the rapid increase in PPFD. However, at low O_2 concentrations, Y(II) in the LL period in fluctuating light did not decrease with the cycles (**Fig. 10**), and no photoinhibition of PSI occurred after the light treatment (**Fig. 11**). These results indicate that an increase in the activity of the CEF-PSI at low O_2 concentrations led to relaxation of the acceptor-side limitation of PSI, resulting in acceleration of the linear and/or the other electron flows. Therefore, we conclude that the CEF-PSI is essential to cope efficiently with the rapid increase in PPFD and prevent photoinhibition of PSI caused by the fluctuating light. Furthermore, our data indicate that the CEF-PSI could be regulated by O_2. The enhancement of the CEF-PSI by low O_2 is probably attributable to suppression of the electron flow to O_2 at low O_2. As the activity of the CEF-PSI cannot be properly regulated in *pgr5*, a considerable number of electrons inevitably flow to O_2, leading to ROS formation and thereby PSI photoinhibition. From these findings, it is suggested that, in the WT, electron flow to O_2 can be controlled by regulating engagement of alternative electron flows including CEF-PSI in such a way that the photooxidative damage is minimized even at 20% O_2.

Apparently, the difference in the responses to the HL periods between the WT and *pgr5* disappeared with the cycles (**Fig. 9**). However, this was due to underestimation of Y(I) that was calculated from the maximal P700 signal, denoted as P_m, because P_m was measured before the fluctuating light treatment. Since P_m decreased greatly in *pgr5* and slightly in the WT due to PSI photoinhibition, there were large differences in the ETR(I)/ETR(II) ratio in the HL period between the WT and *pgr5* when

P_m values corrected for the photodamaged PSI were used (see **Supplementary Fig. S2**).

In *A. thaliana*, NDH-CEF has been suggested to play a complementary role, since the NDH-CEF is not essential for photosynthesis at least under ordinary laboratory conditions, and NDH-deficient mutants of *A. thaliana* grow similarly to the WT (Munekage et al. 2002, Munekage et al. 2004, Okegawa et al. 2008). We measured the responses of an NDH-deficient mutant, *crr2-2*, to the fluctuating light under the same conditions as those use for **Fig. 1** (**Supplementary Fig. S3**). The results in *crr2-2* were almost identical to those in the WT; Y(II) decreased with the cycles, showing similar changes in the ETR(I)/ETR(II) ratio, and PSI was slightly photoinhibited by the fluctuating light treatment. The light dependence of the ETR(I)/ETR(II) ratio exhibited trends similar to those in the WT. Moreover, at any PPFD, the ratios at 2.7% and 0% O_2 were higher than that at 0% O_2 (**Supplementary Fig. S4**). Thus, we conclude that the NDH-CEF would not contribute to the response to the fluctuating light. It is noteworthy, however, that ETR(I)/ETR(II) ratios in the WT and *pgr5* at the two lowest PPFD levels were somewhat greater than those at 35 μmol $m^{-2}s^{-1}$ (**Fig. 8**). This was not the case in *crr2-2*, although we did not measure the ratios at very low PPFDs for *crr2-2*. These differences may indicate that NDH-CEF in the WT and *pgr5* operated at very low PPFDs, as suggested for *Oryza sativa* (Yamori et al. 2011) and *Marchantia polymorpa* (Ueda et al. 2012). It is necessary to conduct detailed measurements including f_{PSII} with *crr2-2*.

Concluding remarks and future scopes

PSI of the *pgr5* plant was sensitive, as previously reported (Munekage et al. 2008), due to the large acceptor-side limitation of PSI. *pgr5* was particularly sensitive to the fluctuating light, and showed marked photoinhibition of PSI. In this study, we clearly elucidated that *pgr5* can drive CEF-PSI in low light. Namely, *pgr5* not only possesses the capacity for CEF-PSI (Nandha et al. 2007) but actually drives the CEF-PSI at low PPFDs. However, its capacity dramatically decreases with the increase in the PPFD, supporting the view that the PGR5 protein is involved in the redox control of PSI (Nandha et al. 2007).

The general message of this study is that the CEF-PSI is essential for effective responses to drastic light fluctuation. When plants are exposed to drastic fluctuation in PPFD in the field, they would activate the CEF-PSI more than the WWC to accommodate the electron flows and thereby avoid the risk of photo-oxidative damage. We also found that the fluctuation in PPFD is a potent stress factor, even when the PPFD level in the HL periods is moderate.

Plants grown in the forest understorey are exposed to drastic fluctuations in PPFD. If they are able to acclimate to such fluctuating light conditions, one of the mechanisms would be an enhancement of the ability for appropriate regulation of the activity of the CEF-PSI in response to light fluctuation. This would be achieved by the increase in the proportion of the PSI complex with the PGR5 protein. Plants may be able to avoid photodamage to PSI by altering the ratio of the two photosystems in the thylakoid membranes (Jahns and Junge 1992, Yin and Johnson 2000, Suorsa et al. 2012) as observed in *pgr5* grown in constant light in this study. We are currently examining whether the photosynthetic apparatus in the WT acclimates to the drastically fluctuating growth light to actually become resistant to the fluctuating light.

Materials and Methods

Plant materials

Arabidopsis thaliana WT (ecotype Columbia *gl1*) and *pgr5* mutant (Munekage et al. 2002) plants were pot grown in a growth cabinet with white fluorescent light at 90–100 μmol photons $m^{-2}s^{-1}$ for an 8 h photoperiod at room temperature of 23°C and relative humidity of 60%. Plants were irrigated 2–3 times weekly and were fertilized with Hyponex 6-10-5 solution (Hyponex Japan) diluted to 1 : 1,000 strength at every irrigation from 2 weeks after germination. Mature rosette leaves from 7- to 9-week-old plants were used in the experiments.

Chl fluorescence and 830 nm absorbance change measurements

Chl fluorescence and absorption changes at 830 nm were measured simultaneously using a Dual-PAM-100 (Chl fluorescence and P700 absorption analyzer equipped with a P700 dual wavelength emitter at 830 and 875 nm; Walz) with the intact leaf in a hand-made leaf chamber. The CO_2 concentration in the leaf chamber was monitored with a LI-6400 (Li-Cor). The O_2 concentration in the air was controlled by mixing N_2 gas and O_2 gas using mass flow controllers. Saturation pulses (SPs) from red light-emitting diodes (LEDs; >8,000 μmol photons $m^{-2}s^{-1}$, 400 ms duration) were applied to determine the maximum Chl fluorescence with closed PSII centers in the dark (F_m) and in the actinic light (F_m'). The maximum photochemical quantum yield of PSII (F_v/F_m) and effective quantum yield of PSII [Y(II)] were calculated as $(F_m - F_0)/F_m$ and $(F_m' - F_s')/F_m'$ (Genty et al. 1989), respectively, where F_s' is the steady-state Chl fluorescence level in the actinic light from red LEDs with a wavelength peak at 635 nm, in which chloroplast avoidance movement does not occur and has no effect on assessment of non-photochemical quenching components (Cazzaniga et al. 2013). The coefficient of non-photochemical quenching, qN, was calculated as $(F_m - F_m')/(F_m - F_0')$. F_0' is the minimal fluorescence yield in actinic light and was estimated using the approximation of Oxborough and Baker (1997) as $F_0/(F_v/F_m + F_0/F_m')$. Two other PSII quantum yields, Y(NPQ) and Y(NO) (Genty et al. 1996, Kramer et al. 2004b), which represent the regulated and non-regulated energy dissipation at PSII centers, respectively, and add up to unity with the photochemical quantum yield [i.e. Y(II) + Y(NPQ) + Y(NO) = 1], were also used. Y(NPQ) and Y(NO) were calculated as $F_s'/F_m' - F_s'/F_m$ and F_s'/F_m, respectively

(Hendrickson et al. 2004, Klughammer and Schreiber 2008a). The coefficient of photochemical quenching, qL, a measure of the fraction of open PSII reaction centers, based on the 'lake model' of PSII antenna pigment organization, was calculated as $(F_m' - F_s')/(F_m' - F_0') \times F_0'/F_s'$ (Kramer et al. 2004b).

In the Dual-PAM-100, $P700^+$ was monitored as the absorption difference between 830 and 875 nm in transmission mode. In analogy to Chl fluorescence yield, the quantum yield of PSI was determined using the SP method (Klughammer and Schreiber 1994, Klughammer and Schreiber 2008b). The maximum level of P700 signal (P700 fully oxidized) in the dark, called the P_m, was determined by application of an SP in the presence of far-red light at the wavelength of 720 nm. The zero P700 signal, P_0, was determined when complete reduction of P700 was induced after the SP in the absence of far-red light. P_m' is the maximal P700 signal in the presence of actinic light induced by the SP. The photochemical quantum yield of PSI, Y(I), was calculated from the complementary PSI quantum yields of non-photochemical energy dissipation, Y(ND) and Y(NA), respectively: $Y(I) = 1 - Y(ND) - Y(NA)$. Y(ND) corresponds to the fraction of P700 that is already oxidized by actinic light, and Y(NA) corresponds to the fraction of P700 that cannot be oxidized by an SP to the overall P700. These calculations were made according to Klughammer and Schreiber (2008b). To oxidize the intersystem electron carriers, far-red light was applied from 100 ms before the start of the SP to its cessation. As shown in **Fig. 2**, Y(I) did not decrease under constant HL. Our preliminary checks showed that an SP of 400 ms duration was enough to induce maximal $P700^+$ oxidation level and to obtain complete reduction of the level of P700 after the SP. Photodamage by the SP did not occur.

The proportions of the non-photochemical quenching components were determined from the relaxation kinetics of the variable fluorescence (F_v) in the absence of actinic light for 30 min (Quick and Stitt 1989, Walters and Horton 1991). Relaxation of F_v was monitored with SPs given every 100 s to the leaf. The intervals of 100 s were sufficient to eliminate an effect of the SP on F_v relaxation. The fast-relaxing component of fluorescence quenching was assigned to the energy-dependent mechanism (qE), the intermediate relaxing component was assigned to the state transition (qT) and the slow relaxing component was assigned to the photoinhibitory processes (qI). For quantification of qE, qT and qI, the semi-logarithmic plot of F_v vs. time was analyzed considering the relationship $(1 - qN) = (1 - qE) \times (1 - qT) \times (1 - qI)$.

We estimated the electron transport rate through PSI [ETR(I)] and PSII [ETR(II)] simultaneously. In this study, a source of artifacts should be considered for a comparison of ETR(I) with ETR(II). With the blue measuring light, the Chl fluorescence signal mainly emitted from the upper layer of the mesophyll cells closest to the emitter detector unit was detected, while the P700 signal detected was more generally from the whole leaf tissue. In HL, these upper cells would be more prone to light saturation of photosynthesis and photoinhibition than the cells in the deeper layer (Terashima et al. 2009, Oguchi et al. 2011a, Oguchi et al. 2011b). To prevent this preferential light saturation of photosynthesis and photoinhibition near the leaf surface effectively, red light at 635 nm peak wavelength instead of blue light was used as the actinic light. The red actinic light at this wavelength reaches the deeper cell layers, and would cause more even light saturation of photosynthesis and photoinhibition than the blue actinic light.

PSI fluorescence may contribute to total leaf fluorescence (Pfundel 1998, Rappaport et al. 2007). In this study, blue light at 460 nm peak wavelength was used as the measuring light, except for the data shown in **Fig 5**; see below. The blue measuring light excites PSII more than PSI. In addition, according to Pfundel et al. (2013), emission of PSI fluorescence by the *A. thaliana* leaves is low irrespective of growth PPFD levels.

The P700 signal can be interfered with by the absorbance changes of plastocyanin. Up to 10% of the P700 difference in absorption signal measured by the Dual-PAM instrument may be attributable to plastocyanin, which shows considerable absorption at both 830 and 870 nm (Kirchhoff et al. 2004). Livingston et al. (2010) compared the results with the Dual-PAM system and those using the two-wavelength deconvolution method (ΔA of 820–950 nm) described by Oja et al. (2004) and concluded that absorbance changes from plastocyanin or other components may not substantially affect the P700 measurements.

Measurements of the share of absorbed light energy allocated to PSII

To estimate the share of absorbed light energy allocated to PSI and PSII, simultaneous measurements of O_2 evolution and Chl fluorescence in the leaf were made at 23°C using a leaf disk oxygen electrode system (LD2, Hansatech) and a Chl fluorometer (PAM-2500, Walz).

Leaf segments were placed in the chamber of the leaf disk O_2 electrode. When the steady-state rate of O_2 evolution was attained, the quantum yield of PSII photochemistry [Y(II)] was measured. The irradiance of the actinic light was increased in a stepwise manner. A Björkman-type lamp equipped with a red color filter of the wavelength centered at 635 nm was used as the light source. The red light was used to mimic the spectrum of the actinic light of the Dual-PAM system. PPFD was altered with neutral density filters (Toshiba). The air in the chamber contained about 5% CO_2 and 15% O_2. The quantum yield of O_2 evolution [$Y(O_2)$] of the leaf was calculated by dividing the rate of gross O_2 evolution per leaf area (μmol O_2 m^{-2} s^{-1}) by absorbed PPFD. The absorptance of the leaf was measured with a hand-made integrating sphere, whose inside was coated with $BaSO_4$, and a quantum sensor (LI-190SA, Li-Cor). When f_{PSII}, the share of absorbed light energy allocated to PSII, is <0.5, the relationship between the quantum yield of O_2 evolution at saturating CO_2 [$Y(O_2)$] and that of PSII electron transport [Y(II)] can be expressed as $Y(O_2) = I_A \times f_{PSII} \times Y(II)/4$, where I_A is the absorbed PPFD (Genty et al. 1989).

This equation, which compares gross O_2 evolution from the whole tissue with Y(II) obtained from the shallow part of the

mesophyll, may lead to uncertainty in f_{PSII}. The error in f_{PSII} gives rise to uncertainty in ETR(II). Since fluorometrically estimated ETR(II) tends to be underestimated compared with that calculated from the gross O_2 evolution rate, especially at high PPFDs, the ETR(I)/ETR(II) ratio calculated with fluorometrical ETR(II) would be overestimated (Kou et al. 2013). To obtain a Chl fluorescence signal from the deeper mesophyll cells with the PAM-2500, we used red light with a peak at 630 nm as the measuring light. The use of the red measuring light, rather than blue light, would minimalize the error in estimation of the ETR(II), particularly that at relatively low PPFDs. Thus, we used data points obtained at low PPFDs. Effects of fluorescence from PSI would be small at low PPFDs.

Determination of Chl content

Chl *a* and *b* contents were determined according to Porra et al. (1989).

Supplementary data

Supplementary data are available at PCP online.

Funding

This work was supported by the Ministry of Education, Culture, Sports, Science and Technology, Japan [Grant-in-Aid for Scientific Research on Innovative Areas (21114007)].

Acknowledgments

We thank Professor Toshiharu Shikanai for providing the *pgr5* and wild-type Columbia type *gl1* seeds, and Professors Kintake Sonoike, Masahiko Ikeuchi, Chikahiro Miyake and Toshiharu Shikanai, and anonymous reviewers for helpful discussions. We would like to dedicate this paper to the late Professor Kozi Asada who passed away on 15 December 2013.

Disclosures

The authors have no conflicts of interest to declare.

References

Allee, W.C. (1926) Measurement of environmental factors in the tropical rain-forest of Panama. *Ecology* 7: 273–302.

Allen, J. (2002) Photosynthesis of ATP—electrons, proton pumps, rotors, and poise. *Cell* 110: 273–276.

Alter, P., Dreissen, A., Luo, F. and Matsubara, S. (2012) Acclimatory responses of *Arabidopsis* to fluctuating light environment: comparison of different sunfleck regimes and accessions. *Photosynth. Res.* 113: 221–237.

Arnon, D.I. and Chain, R.K. (1975) Regulation of ferredoxin-catalyzed photosynthetic phosphorylations. *Proc. Natl Acad. Sci. USA* 72: 4961–4965.

Arnon, D.I. and Chain, R.K. (1979) Regulatory electron transport pathways in cyclic photophosphorylation: reduction of C-550 and cytochrome b6 by ferredoxin in the dark. *FEBS Lett.* 102: 133–138.

Asada, K. (1999) The water–water cycle in chloroplasts: scavenging of active oxygens and dissipation of excess photons. *Annu. Rev. Plant Physiol. Plant Mol. Biol.* 50: 601–639.

Asada, K. (2000) The water–water cycle as alternative photon and electron sinks. *Philos. Trans. R. Soc. B: Biol. Sci* 355: 1419–1431.

Asada, K., Heber, U. and Schreiber, U. (1993) Electron flow to the intersystem chain from stromal components and cyclic electron flow in maize chloroplasts, as detected in intact leaves by monitoring redox change of P700 and chlorophyll fluorescence. *Plant Cell Physiol.* 34: 39–50.

Björkman, O. and Demmig, B. (1987) Photon yield of O_2 evolution and chlorophyll fluorescence characteristics at 77 K among vascular plants of diverse origins. *Planta* 170: 489–504.

Burrows, P.A., Sazanov, L.A., Svab, Z., Maliga, P. and Nixon, P.J. (1998) Identification of a functional respiratory complex in chloroplasts through analysis of tobacco mutants containing disrupted plastid ndh genes. *EMBO J.* 17: 868–876.

Cazzaniga, S., Dall'Osto, L., Kong, S., Wada, M. and Bassi, R. (2013) Interaction between avoidance of photon absorption, excess energy dissipation and zeaxanthin synthesis against photoxidative stress in Arabidopsis. *Plant J.* 76: 568–579.

Chazdon, R.C. (1988) Sunflecks and their importance to forest understory plants. *Adv. Ecol. Res.* 18: 1–63.

Choi, S.M., Jeong, S.W., Jeong, W.J., Kwon, S.Y., Chow, W.S. and Park, Y. (2002) Chloroplast Cu/Zn-superoxide dismutase is a highly sensitive site in cucumber leaves chilled in the light. *Planta* 216: 315–324.

Chow, W.S. and Hope, A.B. (2004) Electron fluxes through photosystem I in cucumber leaf discs probed by far-red light. *Photosynth. Res.* 81: 77–89.

DalCorso, G., Pesaresi, P., Masiero, S., Aseeva, E., Schünemann, D., Finazzi, G. et al. (2008) A complex containing PGRL1 and PGR5 is involved in the switch between linear and cyclic electron flow in Arabidopsis. *Cell* 132: 273–285.

Evans, G.C. (1956) An area survey method of investigating the distribution of light intensity in woodlands, with particular reference to sunflecks. *J. Ecol.* 44: 391–428.

Fan, D.Y., Nie, Q., Hope, A.B., Hillier, W., Pogson, B.J. and Chow, W.S. (2007) Quantification of cyclic electron flow around Photosystem I in spinach leaves during photosynthetic induction. *Photosynth. Res.* 94: 347–57.

Foyer, C.H. and Noctor, G. (2000) Oxygen processing in photosynthesis: regulation and signalling. *New Phytol.* 146: 359–388.

Genty, B., Briantais, J.M. and Baker, N.R. (1989) The relationship between the quantum yield of photosynthetic electron transport and quenching of chlorophyll fluorescence. *Biochim. Biophys. Acta* 990: 87–92.

Genty, B., Harbinson, J., Cailly, A.L. and Rizza, F. (1996) Fate of excitation at PS II in leaves: the non-photochemical side. Presented at The Third BBSRC Robert Hill Symposium on Photosynthesis, March 31 to April 3, 1996 University of Sheffield, Department of Molecular Biology and Biotechnology, Western Bank, Sheffield, UK, Abstract no. 28.

Hendrickson, L., Furbank, R.T. and Chow, W.S. (2004) A simple alternative approach to assessing the fate of absorbed light energy using chlorophyll fluorescence. *Photosynth. Res.* 82: 73–81.

Herbert, S.K., Fork, D.C. and Malkin, S. (1990) Photoacoustic measurements in vivo of energy storage by cyclic electron flow in algae and higher plants. *Plant Physiol.* 94: 926–934.

Hertle, A.P., Blunder, T., Wunder, T., Pesaresi, P., Pribil, M., Armbruster, U. et al. (2013) PGRL1 is the elusive ferredoxin-plastoquinone reductase in photosynthetic cyclic electron flow. *Mol. Cell* 49: 511–523.

Jahnst, P. and Junge, W. (1992) Thylakoids from pea seedlings grown under intermittent light: biochemical and flash-spectrophotometric properties. *Biochemistry* 31: 7390–7397.

Joet, T., Cournac, L., Peltier, G. and Havaux, M. (2002) Cyclic electron flow around photosystem I in C_3 plants. In vivo control by the redox state of chloroplasts and involvement of the NADH-dehydrogenase complex. *Plant Physiol.* 128: 760–769.

Johnson, G.N. (2011) Physiology of PSI cyclic electron transport in higher plants. *Biochim. Biophys. Acta* 1807: 384–389.

Joliot, P., Béal, D. and Joliot, A. (2004) Cyclic electron flow under saturating excitation of dark-adapted Arabidopsis leaves. *Biochim. Biophys. Acta* 1656: 166–176.

Joliot, P. and Johnson, G.N. (2011) Regulation of cyclic and linear electron flow in higher plants. *Proc. Natl Acad. Sci. USA* 108: 13317–13322.

Joliot, P. and Joliot, A. (2006) Cyclic electron flow in C_3 plants. *Biochim. Biophys. Acta* 1757: 362–368.

Joliot, P. and Joliot, A. (2002) Cyclic electron transfer in plant leaf. *Proc. Natl Acad. Sci. USA* 99: 10209–10214.

Joliot, P. and Joliot, A. (2005) Quantification of cyclic and linear flows in plants. *Proc. Natl Acad. Sci. USA* 102: 4913–4918.

Kirchhoff, H., Schöttler, M.A., Maurer, J. and Weis, E. (2004) Plastocyanin redox kinetics in spinach chloroplasts: evidence for disequilibrium in the high potential chain. *Biochim. Biophys. Acta* 1659: 63–72.

Klughammer, C. and Schreiber, U. (1994) An improved method, using saturating light pulses, for the determination of photosystem I quantum yield via $P700^+$-absorbance changes at 830 nm. *Planta* 192: 261–268.

Klughammer, C. and Schreiber, U. (2008a) Complementary PS II quantum yields calculated from simple fluorescence parameters measured by PAM fluorometry and the Saturation Pulse method. *PAM Application Notes* 1: 27–35.

Klughammer, C. and Schreiber, U. (2008b) Saturation Pulse method for assessment of energy conversion in PS I. *PAM Application Notes* 1: 11–14.

Knapp, A.K. and William, K.S. (1989) Influence of growth form on ecophysiological responses to variable sunlight in subalpine plants. *Ecology* 70: 1069–1082.

Koizumi, H. and Oshima, Y. (1993) Light environment and carbon gain of understory herbs associated with sunflecks in a warm temperate deciduous forest in Japan. *Ecol. Res.* 8: 135–142.

Kou, J., Takahashi, S., Oguchi, R., Badger, M.R. and Chow, W.S. (2013) Estimation of the steady-state cyclic electron fl ux around PSI in spinach leaf discs in white light, CO_2 -enriched air and other varied conditions. *Funct. Plant Biol.* 40: 1018–1028.

Kramer, D.M., Avenson, T.J. and Edwards, G.E. (2004a) Dynamic flexibility in the light reactions of photosynthesis governed by both electron and proton transfer reactions. *Trends Plant Sci.* 9: 349–357.

Kramer, D.M., Johnson, G., Kiirats, O. and Edwards, G.E. (2004b) New fluorescence parameters for the determination of Q_A redox state and excitation energy fluxes. *Photosynth. Res.* 79: 209–218.

Lennon, A.M., Prommeenate, P. and Nixon, P.J. (2003) Location, expression and orientation of the putative chlororespiratory enzymes, Ndh and IMMUTANS, in higher-plant plastids. *Planta* 218: 254–260.

Livingston, A.K., Cruz, J.A., Kohzuma, K., Dhingra, A. and Kramer, D.M. (2010) An Arabidopsis mutant with high cyclic electron flow around photosystem I (hcef) involving the NADPH dehydrogenase complex. *Plant Cell* 22: 221–233.

Makino, A., Miyake, C. and Yokota, A. (2002) Physiological functions of the water–water cycle (Mehler reaction) and the cyclic electron flow around PSI in rice leaves. *Plant Cell Physiol.* 43: 1017–1026.

Maxwell, P.C. and Biggins, J. (1976) Role of cyclic electron transport in photosynthesis as measured by the photoinduced turnover of P700 in vivo. *Biochemistry* 15: 3975–3981.

Miyake, C. (2010) Alternative electron flows (water–water cycle and cyclic electron flow around PSI) in photosynthesis: molecular mechanisms and physiological functions. *Plant Cell Physiol.* 51: 1951–1963.

Miyake, C. and Yokota, A. (2000) Determination of the rate of photoreduction of O_2 in the water–water cycle in watermelon leaves and enhancement of the rate by limitation of photosynthesis. *Plant Cell Physiol.* 41: 335–343.

Müller, P., Li, X. and Niyogi, K.K. (2001) Update on photosynthesis: non-photochemical quenching. A response to excess light energy. *Plant Physiol.* 125: 1558–1566.

Munekage, Y., Genty, B. and Peltier, G. (2008) Effect of PGR5 impairment on photosynthesis and growth in Arabidopsis thaliana. *Plant Cell Physiol.* 49: 1688–1698.

Munekage, Y., Hashimoto, M., Miyake, C., Tomizawa, K., Endo, T., Tasaka, M. et al. (2004) Cyclic electron flow around photosystem I is essential for photosynthesis. *Nature* 429: 579–582.

Munekage, Y., Hojo, M., Meurer, J., Endo, T., Tasaka, M. and Shikanai, T. (2002) PGR5 is involved in cyclic electron flow around photosystem I and is essential for photoprotection in *Arabidopsis*. *Cell* 110: 361–371.

Nandha, B., Finazzi, G., Joliot, P., Hald, S. and Johnson, G.N. (2007) The role of PGR5 in the redox poising of photosynthetic electron transport. *Biochim. Biophys. Acta* 1767: 1252–1259.

Oguchi, R., Douwstra, P., Fujita, T., Chow, W.S. and Terashima, I. (2011a) Intra-leaf gradients of photoinhibition induced by different color lights: implications for the dual mechanisms of photoinhibition and for the application of conventional chlorophyll fluorometers. *New Phytol.* 191: 146–159.

Oguchi, R., Terashima, I., Kou, J. and Chow, W.S. (2011b) Operation of dual mechanisms that both lead to photoinactivation of Photosystem II in leaves by visible light. *Physiol. Plant.* 142: 47–55.

Oja, V., Bichele, I., Hüve, K., Rasulov, B. and Laisk, A. (2004) Reductive titration of photosystem I and differential extinction coefficient of P700+ at 810–950 nm in leaves. *Biochim. Biophys. Acta* 1658: 225–234.

Okegawa, Y., Kagawa, Y., Kobayashi, Y. and Shikanai, T. (2008) Characterization of factors affecting the activity of photosystem I cyclic electron transport in chloroplasts. *Plant Cell Physiol.* 49: 825–834.

Osmond, B., Badger, M., Maxwell, K., Bjorkman, O. and Leegood, R. (1997) Too many photons: photorespiration, photoinhibition and photooxidation. *Trends Plant Sci.* 2: 119–121.

Osmond, B. and Grace, C. (1995) Perspectives on photoinhibition and photorespiration in the field: quintessential inefficiencies of the light and dark reactions of photosynthesis? *J. Exp. Bot.* 46: 1351–1362.

Oxborough, K. and Baker, N.R. (1997) Resolving chlorophyll a fluorescence images of photosynthetic efficiency into photochemical and

non-photochemical components—calculation of qP and F_v'/F_m' without measuring F_o'. *Photosynth. Res.* 54: 135–142.

Pearcy, R.W. (1983) The light environment and growth of C_3 and C_4 trees species in the understory of a Hawaiian forest. *Oecologia* 58: 19–25.

Peng, L., Yamamoto, H. and Shikanai, T. (2011) Structure and biogenesis of the chloroplast NAD(P)H dehydrogenase complex. *Biochim. Biophys. Acta* 1807: 945–953.

Pesaresi, P., Pribil, M., Wunder, T. and Leister, D. (2011) Dynamics of reversible protein phosphorylation in thylakoids of flowering plants: the roles of STN7, STN8 and TAP38. *Biochim. Biophys. Acta* 1807: 887–896.

Pfündel, E. (1998) Estimating the contribution of Photosystem I to total leaf chlorophyll fluorescence. *Photosynth. Res.* 56: 185–195.

Pfündel, E.E., Klughammer, C., Meister, A. and Cerovic, Z.G. (2013) Deriving fluorometer-specific values of relative PSI fluorescence intensity from quenching of F(0) fluorescence in leaves of *Arabidopsis thaliana* and *Zea mays*. *Photosynth. Res.* 114: 189–206.

Porra, R.J., Thompson, W.A. and Kriedemann, P.E. (1989) Determination of accurate extinction coefficients and simultaneous equations for assaying chlorophylls *a* and *b* extracted with four different solvents: verification of the concentration of chlorophyll standards by atomic absorption spectroscopy. *Biochim. Biophys. Acta* 975: 384–394.

Quick, W.P. and Stitt, M. (1989) An examination of factors contributing to non-photochemical quenching of chlorophyll fluorescence in barley leaves. *Biochim. Biophys. Acta* 977: 287–296.

Rappaport, F., Béal, D., Joliot, A. and Joliot, P. (2007) On the advantages of using green light to study fluorescence yield changes in leaves. *Biochim. Biophys. Acta* 1767: 56–65.

Rosso, D., Ivanov, A.G., Fu, A., Geisler-Lee, J., Hendrickson, L., Geisler, M. et al. (2006) IMMUTANS does not act as a stress-induced safety valve in the protection of the photosynthetic apparatus of Arabidopsis during steady-state photosynthesis. *Plant Physiol.* 142: 574–585.

Rott, M., Martins, N.F., Thiele, W., Lein, W., Bock, R., Kramer, D.M. et al. (2011) ATP synthase repression in tobacco restricts photosynthetic electron transport, CO2 assimilation, and plant growth by overacidification of the thylakoid lumen. *Plant Cell* 23: 304–321.

Sacksteder, C.A., Kanazawa, A., Jacoby, M.E. and Kramer, D.M. (2000) The proton to electron stoichiometry of steady-state photosynthesis in living plants: a proton-pumping Q cycle is continuously engaged. *Proc. Natl Acad. Sci. USA* 97: 14283–14288.

Sacksteder, C.A. and Kramer, D.M. (2000) Dark-interval relaxation kinetics (DIRK) of absorbance changes as a quantitative probe of steady-state electron transfer. *Photosynth. Res.* 66: 145–158.

Scheller, H.V. (1996) In vitro cyclic electron transport in barley thylakoids follows two independent pathways. *Plant Physiol.* 110: 187–194.

Schreiber, U., Hormann, H., Asada, K. and Neubauer, C. (1995) O_2-dependent electron flow in spinach chloroplast: properties and possible regulation of the Mehler–ascorbate peroxidase cycle. *In* Photosynthesis: From Light to Biosphere 2. Edited by Mathis, P. pp. 813–818. Academic Press, Dordrecht.

Shikanai, T. (2007) Cyclic electron transport around photosystem I: genetic approaches. *Annu. Rev. Plant Biol.* 58: 199–217.

Shikanai, T., Endo, T., Hashimoto, T., Yamada, Y., Asada, K. and Yokota, A. (1998) Directed disruption of the tobacco ndhB gene impairs cyclic electron flow around photosystem I. *Proc. Natl Acad. Sci. USA* 95: 9705–9709.

Shikanai, T., Munekage, Y., Shimizu, K., Endo, T. and Hashimoto, T. (1999) Identification and characterization of *Arabidopsis* mutants with reduced quenching of chlorophyll fluorescence. *Plant Cell Physiol.* 40: 1134–1142.

Sonoike, K. (1996) Photoinhibition of photosystem I: its physiological significance in the chilling sensitivity of plants. *Plant Cell Physiol.* 37: 239–247.

Sonoike, K., Kamo, M., Hihara, Y., Hiyama, T. and Enami, I. (1997) The mechanism of the degradation of psaB gene product, one of the photosynthetic reaction center subunits of Photosystem I, upon photoinhibition. *Photosynth. Res.* 53: 55–63.

Suorsa, M., Järvi, S., Grieco, M., Nurmi, M., Pietrzykowska, M., Rantala, M. et al. (2012) PROTON GRADIENT REGULATION5 is essential for proper acclimation of *Arabidopsis* photosystem I to naturally and artificially fluctuating light conditions. *Plant Cell* 24: 2934–2948.

Takabayashi, A., Kishine, M., Asada, K., Endo, T. and Sato, F. (2005) Differential use of two cyclic electron flows around photosystem I for driving CO_2-concentration mechanism in C_4 photosynthesis. *Proc. Natl Acad. Sci. USA* 102: 16898–16903.

Tikkanen, M., Grieco, M., Kangasjärvi, S. and Aro, E.M. (2010) Thylakoid protein phosphorylation in higher plant chloroplasts optimizes electron transfer under fluctuating light. *Plant Physiol.* 152: 723–735.

Terashima, I., Fujita, T., Inoue, T., Chow, W.S. and Oguchi, R. (2009) Green light drives leaf photosynthesis more efficiently than red light in strong white light: revisiting the enigmatic question of why leaves are green. *Plant Cell Physiol.* 50: 684–697.

Ueda, M., Kuniyoshi, T., Yamamoto, H., Sugimoto, K., Ishizaki, K. et al. (2012) Composition and physiological function of the chloroplast NADH dehydrogenase-like complex in Marchantia polymorpha. *Plant J.* 72: 683–693.

Vierling, L.A. and Wessman, C.A. (2000) Photosynthetically active radiation heterogeneity within a monodominant Congolese rain forest canopy. *Agric. Forest Meteorol.* 103: 265–278.

Waiters, R.G. and Horton, P. (1991) Resolution of components of non-photochemical chlorophyll fluorescence quenching in barley leaves. *Photosynth. Res.* 27: 121–133.

Yamamoto, H., Peng, L., Fukao, Y. and Shikanai, T. (2011) An Src homology 3 domain-like fold protein forms a ferredoxin binding site for the chloroplast NADH dehydrogenase-like complex in Arabidopsis. *Plant Cell* 23: 1480–1493.

Yamori, W., Sakata, N., Suzuki, Y., Shikanai, T. and Makino, A. (2011) Cyclic electron flow around photosystem I via chloroplast NAD(P)H dehydrogenase (NDH) complex performs a significant physiological role during photosynthesis and plant growth at low temperature in rice. *Plant J.* 68: 966–976.

Yin, Z.H. and Johnson, G.N. (2000) Photosynthetic acclimation of higher plants to growth in fluctuating light environments. *Photosynth. Res.* 63: 97–107.